arXiv:cond-mat/0511553v2 [cond-mat.mes-hall] 5 May 2006

Spectroscopic properties of large open quantum-chaotic cavities with and without separated time scales

Evgeny N. Bulgakov[1,2] and Ingrid Rotter[2]

[1] *Kirensky Institute of Physics, 660036, Krasnoyarsk, Russia and*

[2] *Max Planck Institute for the Physics of Complex Systems, D-01187 Dresden, Germany*

(Dated: February 2, 2008)

Abstract

The spectroscopic properties of an open large Bunimovich cavity are studied numerically in the framework of the effective Hamiltonian formalism. The cavity is opened by attaching two leads to it in four different ways. In some cases, the transmission takes place via standing waves with an intensity that closely follows the profile of the resonances. In other cases, short-lived and long-lived resonance states coexist. The short-lived states cause traveling waves in the transmission while the long-lived ones generate superposed fluctuations. The traveling waves oscillate as a function of energy. They are not localized in the interior of the large chaotic cavity. In all considered cases, the phase rigidity fluctuates with energy. It is mostly near to its maximum value and agrees well with the theoretical value for the two-channel case.

I. INTRODUCTION

During last years, much interest is devoted to the study of the spectral properties of small cavities coupled to a small number of channels. As a function of the coupling strength between cavity and attached leads, the results obtained show the resonance trapping effect in theoretical [1] as well as in experimental [2] studies. Short-lived whispering gallery modes are formed by attaching the leads in a suitable manner to cavities of different shape with convex boundary [3]. These direct processes can result in deterministic transport as signified by a striking system-specific suppression of shot noise [4]. The corresponding pathways are localized inside the cavities: the whispering gallery modes near to the convex boundary and the bouncing ball modes around the shortest pathway between the two attached leads [3].

The whispering gallery modes can be characterized well by classical values such as pathway length and travelling time [3]. The last value is related to the lifetime of the corresponding state, for example to the lifetime of the whispering gallery mode. That means the shorter the pathways of the direct modes, the shorter the lifetimes of the corresponding resonance states and the better these states are separated from the other resonance states of the system by their lifetimes. It follows immediately from these relations that it is easy to identify the whispering gallery modes inside a small system, i.e. in a cavity whose attached leads have a width that is relatively large as compared to the area of the cavity. It might however be difficult to identify them in a large system that is relatively weakly coupled to the leads due to its large area and relatively small width of the attached leads. Here the pathway between the two attached leads is long. The question arises therefore whether or not whispering gallery modes can be identified also in large cavities.

Guided by the results of previous calculations for small cavities [3, 4], we have chosen billiards of Bunimovich type for the study of this question. We opened these billiards by attaching two leads to them and used four different geometries for the positions and orientations of the leads with the aim to study the transmission through the cavity under different conditions. The spectroscopic study is based on the method of the effective non-hermitian Hamilton operator $H_{\rm eff}$ that describes the spectroscopic properties of an open quantum system, i.e. of a quantum system that is opened by embedding it into a common continuum of scattering wave functions [5]. This means in the present case that leads are attached to the closed cavity for the propagation of the scattering wave functions corresponding to

one channel in each lead. In some of the open cavities, the expectation value $\langle t(E)\rangle$ of the transmission amplitude $t(E)$ shows an oscillatory behaviour. The oscillation length depends on the geometry of the attached leads. It may be large for bouncing ball modes when the distance between the input and output leads is small. It is however much smaller in the case of the whispering gallery modes that appear in a small attached half stadium and are characterized by a relatively large distance between the input and output leads.

The paper is organized in the following manner. In Sec. II, we provide a few of the basic equations that describe the different time scales in open quantum systems. The time scales are determined by the lifetimes of the resonance states which are obtained from the eigenvalues of the effective Hamiltonian $H_{\rm eff}$ that describes the open quantum system. They depend on the manner the leads are attached to the quantum billiard. We show further the results of numerical simulations for the transmission through the four different cavities. In the case of whispering gallery modes and bouncing ball modes between the two attached leads, $\langle t(E)\rangle$ oscillates with a period that is determined by the momentum k and the geometry of the open cavity. In Sec. III, we consider the eigenfunctions of the effective Hamiltonian. The eigenfunctions are biorthogonal with the consequence that, in the regime of overlapping resonances, the real and imaginary parts of the eigenfunctions may decouple, to a certain degree. We relate this decoupling to the phase rigidity of the scattering wave function which expresses the distortion of the scattering wave function by the overlapping of the different resonance states. As for the transmission, we calculate the expectation value of the phase rigidity. For isolated resonances, the real and imaginary parts of the eigenfunctions are related to one another in the standard manner and the transmission takes place by standing waves. In the overlapping regime, however, the real and imaginary parts of the eigenfunctions decouple from one another and eventually traveling waves arise. When fully evolved, the traveling waves are superposed by long-lived standing waves. The traveling waves are described by the so-called optical S matrix. The results are summarized in the last section.

II. EIGENVALUES OF THE EFFECTIVE HAMILTONIAN AND SEPARATED TIME SCALES

A. Eigenvalues and transmission

The energies and widths of the resonance states of an open quantum system can be obtained from the poles of the S matrix or directly from the eigenvalues z_k of the corresponding effective Hamilton operator $H_{\rm eff}$ [5]. For a quantum billiard with two attached leads, the effective Hamiltonian is [6]

$$H_{\rm eff} = H_B + \sum_{C=R,L} V_{BC} \frac{1}{E^+ - H_C} V_{CB} \tag{1}$$

where H_B is the Hamiltonian of the closed quantum billiard, H_C is the Hamiltonian of the left ($C = L$) and right ($C = R$) lead and $E^+ = E + i0$. The second term of $H_{\rm eff}$ takes into account the coupling of the *eigenstates* of H_B via the modes propagating in the leads when the system is opened. It introduces correlations between the states of an open quantum system which appear *additionally* to those of the closed system [5]. The (real) eigenvalues E_λ^B of the Hamiltonian H_B are the energies of the discrete states of the closed system, while the (complex) eigenvalues z_λ of $H_{\rm eff}$ provide the positions E_λ and widths Γ_λ of the corresponding resonance states of the open system. There is a one-to-one correspondence between the number of eigenstates of H_B and that of $H_{\rm eff}$.

Since the effective Hamiltonian (1) depends explicitely on the energy E, so do its eigenvalues z_λ. The energy dependence is small, as a rule, in an energy interval that is determined by the width of the resonance state. The solutions of the fixed-point equations

$$E_\lambda = {\rm Re}(z_\lambda)_{|E=E_\lambda} \tag{2}$$

and of

$$\Gamma_\lambda = -2\,{\rm Im}(z_\lambda)_{|E=E_\lambda} \tag{3}$$

are numbers that coincide approximately with the poles of the S matrix. The width Γ_λ determines the time scale characteristic of the resonance state λ. The amplitude for the transmission in the one-channel case is [6]

$$t = -2\pi i \sum_\lambda \frac{\langle \xi_L^E | V | \phi_\lambda)(\phi_\lambda | V | \xi_R^E \rangle}{E - z_\lambda} \tag{4}$$

where the eigenfunctions of $H_{\rm eff}$ are denoted by ϕ_λ and the scattering wave functions in the leads by ξ_C^E. According to (4), the transmission is *resonant* in relation to the effective Hamiltonian $H_{\rm eff}$. This holds for narrow resonance states as well as for the short-lived and long-lived resonance states that appear after redistribution of the spectroscopic properties of the system. Such a redistribution is studied first numerically in a nucleus [7] and then analytically, by using statistical assumptions and neglecting the energy dependence of the z_λ, in a large chaotic system [8]. It is caused by branch points in the complex energy plane [9]. That means, the eigenvalues z_λ of $H_{\rm eff}$ determine the time scale of the transmission.

The coupling matrix elements $V_{BC},\ V_{CB}$ between billiard and attached leads can be calculated in the tight-binding approach [6, 10]. When they are small, it is $E_\lambda \approx E_\lambda^0$ and $\Gamma_\lambda \approx \Gamma_\lambda^0$ where E_λ^0 is the position of the isolated resonance state and Γ_λ^0 its width that is determined by the $V_{BC},\ V_{CB}$. For large $V_{BC},\ V_{CB}$, however, E_λ^0 and E_λ as well as Γ_λ^0 and Γ_λ may be very different from one another due to reordering processes taking place in the system at strong coupling to the environment (full opening of the quantum billiard). In this regime, short-lived and long-lived resonance states coexist [5]. Examples are short-lived bouncing ball modes or whispering gallery modes that may coexist with long-lived resonance states in a small quantum billiard [3].

Whispering gallery modes may appear in small chaotic as well as regular billiards with convex boundary when fully opened *and* the leads are attached to them in a suitable manner. Examples are billiards of Bunimovich and circular type [3]. The whispering gallery modes are localized near to the boundary of the billiard. They have an approximately equal distance in momentum k from one another, and their positions in energy are determined by the number of nodes which increases with increasing energy. The widths are proportional to the length of the pathway along the convex boundary (except for threshold effects) [3]. A shot-noise analysis has shown that they support direct transport processes [4]. They determine, therefore, the optical S matrix. The long-lived states however feature indeterministic processes corresponding to the universal prediction of random matrix theory [4]. They cause the fluctuations of the transmission probability.

B. Numerical simulation

In this section, we show the results of numerical simulations for the transmission through a cavity of Bunimovich type with leads attached in four different ways. The calculations for the transmission are performed by using the boundary element method [11]. The eigenvalues of $H_{\rm eff}$ are obtained by applying the tight-binding lattice Green function method given in Ref. [12] and using the general relation between $H_{\rm eff}$ and the Green function. The energies and widths of the resonance states are obtained by solving the fixed-point equations (2) and (3). The ensemble average $\langle t \rangle$ is performed from 200 different positions of an internal obstacle by keeping fixed the area of the billiard. The energy interval considered is divided usually into 20 energy bins.

In Fig. 1, we show the ensemble expectation values $\langle t(E) \rangle$ of the transmission as a function of the energy E in the region $E = 14 - 26$ for the four cavities shown in the insets of Fig. 2. The oscillating contribution from the short-lived states as well as the shifts between $\mathrm{Re}\langle t(E) \rangle$ and $\mathrm{Im}\langle t(E) \rangle$ can be seen clearly in the cavities (c) and (d). Interesting is the geometry of the cavity (b) where the transmission $\langle t(E) \rangle$ changes its nature at $E \approx 21$.

In Fig. 2, we show the eigenvalues of the effective Hamiltonian (1) for the four cavities. The values E_λ and Γ_λ of the short-lived states are calculated by solving the fixed-point equations (2) and (3). We have resonance states with well separated time scales in Figs. 2(c) and (d). In these cases, $\langle t(E) \rangle$ is large and oscillates. In Fig. 2(a), separated time scales can not be identified and $\langle t(E) \rangle$ is relatively small. In Fig. 2(b), separated time scales can be identified but the difference between the short-lived and the long-lived states is smaller than in (c) and (d). Furthermore, the widths of the long-lived states are spread in (b) over a comparably large range and the widths of the short-lived states show an irregularity around $E \approx 21$. At this energy, $\langle t(E) \rangle$ changes its nature as can be seen from Fig. 1 (b). In any case, Figs. 1(b) and 2(b) show that the sensitivity of $\langle t(E) \rangle$ against parameter variations is large when the direct pathway between the input and output leads is large and not well separated from other pathways through the interior of the cavity. This sensitivity can be seen also in comparing the results for the cavities (a) and (d). While there is almost no separation of the pathways through the small attached half stadium from those through the large Bunimovich stadium in (a), both parts are well separated in (d). As a consequence, we see whispering gallery modes in the small attached stadium in (d) but not in (a).

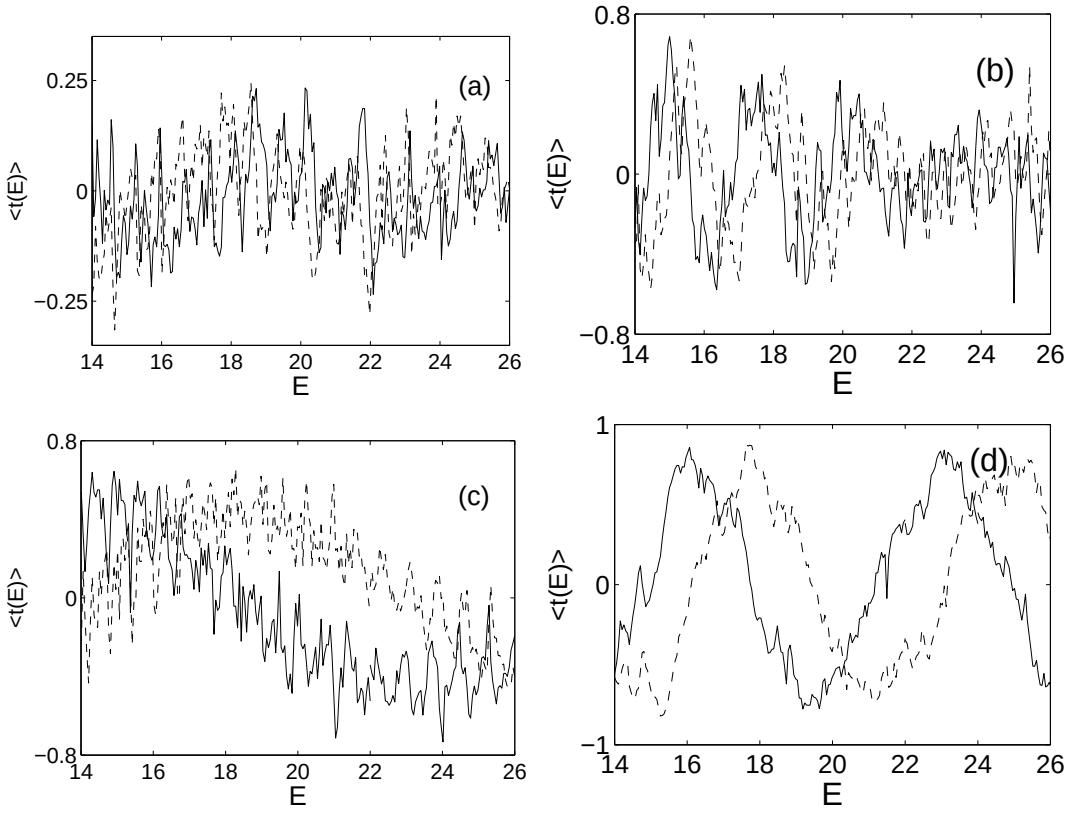

FIG. 1: The ensemble expectation value $\langle t(E)\rangle$ as a function of the energy E for the cavities (a), (b), (c) and (d) shown in the insets of Fig. 2. The cavities consist of a Bunimovich stadium connected to two waveguides directly, as in panels (a), (b) and (c), or through a smaller half stadium, as in (d). Full lines: $\mathrm{Re}\langle t(E)\rangle$, dashed lines: $\mathrm{Im}\langle t(E)\rangle$. Most $\langle t(E)\rangle$ show oscillations that are related to the distances between the input and output leads. The energy is in units $\hbar^2/2m$ and $d = 1$ is the width of the wave guide.

The short-lived states determine the value of the so-called optical S matrix.

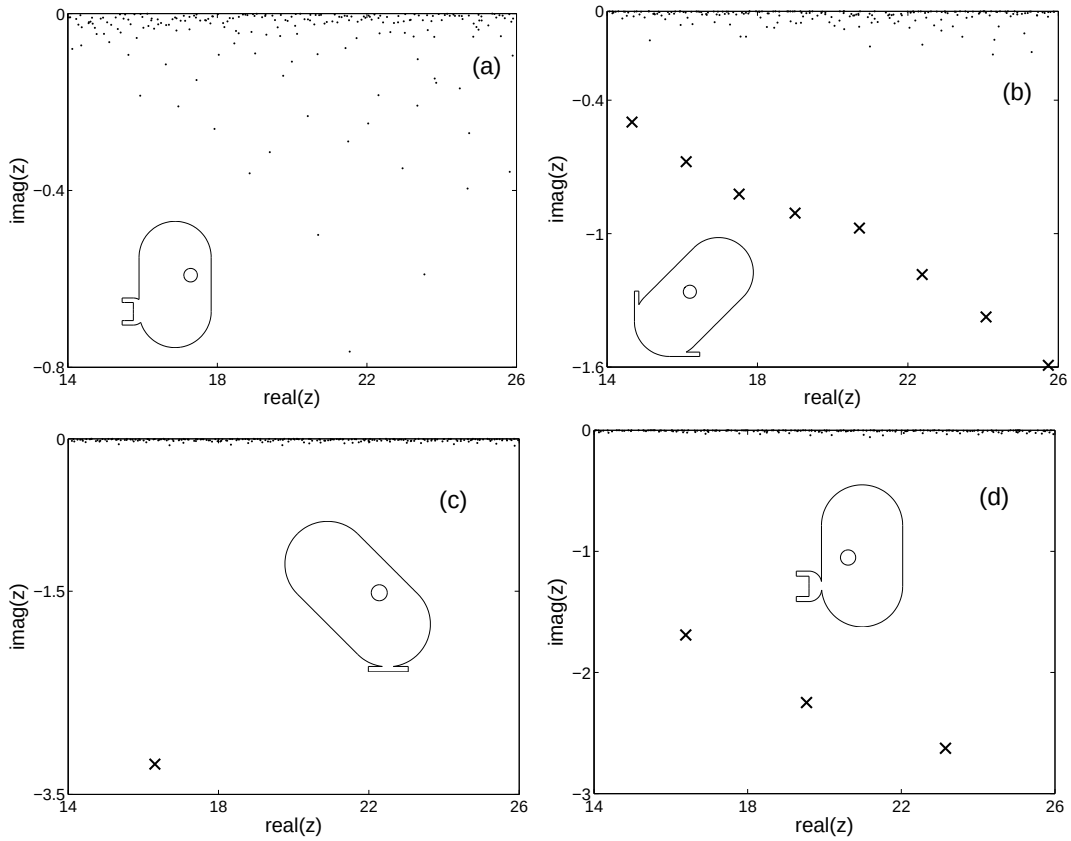

FIG. 2: The solutions of the fixed-point equations (2) and (3) for the resonance states of the four different cavities. The short-lived states are marked by crosses, the long-lived ones by dots. A clear separation of the time scales can be seen in (c) and (d). The neighboring short-lived resonance state in (c) lies at $E_\lambda - i/2\ \Gamma_\lambda = 27.74 - 6.89\ i$. In the insets, the cavities are shown. In order to see the differences between the four open cavities, the attached leads are also shown up to an arbitrary distance L. The eigenvalues are calculated with $L = 0$.

III. EIGENFUNCTIONS OF THE EFFECTIVE HAMILTONIAN AND PHASE RIGIDITY

A. Eigenfunctions and transmission

The scattering wave function Ψ_C^E is solution of the Schrödinger equation $(H - E)\Psi_C^E = 0$ in the total function space with the hermitian Hamilton operator H. It reads [5, 6]

$$\Psi_C^E = \xi_C^E + \sum_\lambda \left[\phi_\lambda \,+\, \xi_C^E \,\frac{1}{E^+ - H_C}\,\langle \xi_C^E | V | \phi_\lambda \rangle\right] \frac{(\phi_\lambda | V | \xi_C^E \rangle}{E - z_\lambda}\,. \tag{5}$$

The ϕ_λ are complex and biorthogonal [5],

$$(\phi_\lambda|\phi_{\lambda'}) \equiv \langle\phi_\lambda^*|\phi_{\lambda'}\rangle = \delta_{\lambda,\lambda'} \tag{6}$$

$$|\langle\phi_\lambda|\phi_\lambda\rangle| = A_\lambda \geq 1\,; \qquad |\langle\phi_\lambda|\phi_{\lambda'}\rangle| = B_\lambda^{\lambda'} \geq 0\,. \tag{7}$$

Eq. (5) shows that the scattering wave function Ψ_C^E in the interior region of the quantum dot is determined, above all, by the complex eigenfunctions ϕ_λ of $H_{\rm eff}$,

$$\Psi_C^E(r) \to \sum_\lambda \phi_\lambda(r)\,\frac{(\phi_\lambda|V|\xi_C^E\rangle}{E - z_\lambda}\,. \tag{8}$$

At the energy $E \approx E_\lambda$, the eigenfunction $\phi_\lambda(r)$ of the effective Hamiltonian $H_{\rm eff}$ gives the main contribution. This holds true especially at the energy of a narrow resonance state. As a numerical example, the eigenfunction ϕ_λ of a whispering gallery mode is shown in Fig. 3 for the cavity (d) and compared with the corresponding scattering wave function Ψ_C^E at the energy E_λ. The scattering wave function contains contributions from other eigenfunctions also at $E = E_\lambda$. Nevertheless, it shows, at this energy, the typical structure of the whispering gallery mode. As can be seen from the figure, it is localized not inside the large Bunimovich cavity but outside of it in the small half stadium.

The real and imaginary parts of the eigenfunctions ϕ_λ are more or less decoupled in the regime of overlapping resonances [13]. The value

$$r_\lambda \;=\; \Big|\frac{\int dr(|{\rm Re}\,\phi_\lambda(r)|^2 - |{\rm Im}\,\phi_\lambda(r)|)^2}{\int dr(|{\rm Re}\,\phi_\lambda(r)|^2 + |{\rm Im}\,\phi_\lambda(r)|)^2}\Big| = \Big|\frac{(\phi_\lambda|\phi_\lambda)}{\langle\phi_\lambda|\phi_\lambda\rangle}\Big| = \frac{1}{A_\lambda} \tag{9}$$

is a measure for the biorthogonality of the eigenfunctions of $H_{\rm eff}$. The phase rigidity $|\rho|^2$ of the scattering wave function $\Psi(r)$ is considered in e.g. Refs. [14, 15],

$$\rho = \frac{\int dr\ \Psi(r)^2}{\int dr\ |\Psi(r)|^2} = e^{2i\theta}\frac{\int dr\ (|{\rm Re}\tilde{\Psi}(r)|^2 - |{\rm Im}\tilde{\Psi}(r)|^2)}{\int dr\ (|{\rm Re}\tilde{\Psi}(r)|^2 + |{\rm Im}\tilde{\Psi}(r)|^2)} \tag{10}$$

where θ is an angle providing that ${\rm Re}\tilde{\Psi}(r)$ and ${\rm Im}\tilde{\Psi}(r)$ are orthogonal. The value ρ is related to the r_λ according to (8).

For an isolated resonance state, $A_\lambda \approx 1$ and $r_\lambda \approx 1$ at the energy $E = E_\lambda$. At this energy, the transmission probability shows a peak. Approaching a branch point in the complex energy plane [5] where two eigenvalues z_{λ_1} and z_{λ_2} coalesce, $A_\lambda \to \infty$ and $r_\lambda \to 0$ [13, 16]. Here, the widths bifurcate : one of the states aligns with the channel wave function and becomes short-lived while the other one becomes long-lived [5]. Eventually, the short-lived

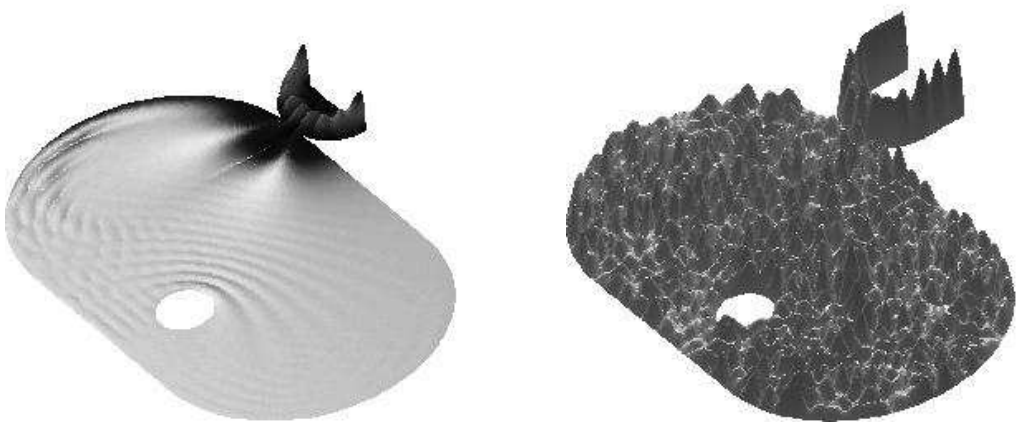

FIG. 3: The eigenfunction ϕ_λ of the effective Hamiltonian $H_{\rm eff}$ at the energy $E = E_\lambda$ of the whispering gallery mode λ (left) and the scattering wave function Ψ_C^E at the same energy E (right). $E_\lambda - i/2\ \Gamma_\lambda = 19.53 - 2.25\ i$. The ϕ_λ is shown up to the attached lead ($L = 0$) while the Ψ_C^E is shown, for illustration, also in the lead up to an arbitrary finite value L.

and long-lived resonance states differ strongly from one another and do not cross in the complex energy plane [13]. Therefore again, as for non-overlapping resonances, $A_\lambda \to 1$ and $r_\lambda \to 1$ at the energies $E = E_\lambda$ of the long-lived states. In the transmission through the cavity, the short-lived states determine the smooth 'background' while the long-lived states cause the superposed peaks (fluctuations) in the transmission probability [9].

This picture can be translated to that of 'standing' and 'traveling' waves. Standing waves

$$\psi(r) = (2N)^{-1/2} \sum_{n=1}^{N} \cos\ [(\theta_n + k_n \cdot r)] \tag{11}$$

cause the Porter-Thomas statistics for the intensity [17]. Tuning the frequency to a resonance, an intensity pattern is generated that closely follows the profile of this resonance. In this situation, the resonances are isolated from one another and $A_\lambda \to 1$, $r_\lambda \to 1$.

When the cavity is fully open, the local field can be viewed as a sum of a number of traveling modes ariving at a point from various scattering processes [17],

$$\psi(r) = (2N)^{-1/2} \sum_{n=1}^{N} \exp\ [i(\theta_n + k_n \cdot r)] \tag{12}$$

where the phases θ_n are completely random and the wave vectors k_n are uniformly distributed. Both $\mathrm{Re}(\psi)$ and $\mathrm{Im}(\psi)$ are independent Gaussian variables what leads to the

Rayleigh distribution for the intensity $I(r) \equiv |\psi(r)|^2$. It applies to a monochromatic wave propagating in an open system ('traveling wave' excited by a monochromatic source [17]). In the corresponding description of this situation with the effective Hamiltonian formalism, short-lived and long-lived resonance states coexist in the system and determine, respectively, the smooth 'background' and the superposed peaks (fluctuations) of the transmission probability [9]. The short-lived resonance states are strongly related to the channel wave functions (scattering states in the leads) due to the large overlap integral of their wave functions with those of the channel wave functions. The transmission induced by these states shows therefore the same dependence on the momentum k as the scattering wave functions ξ_C^E in the leads ('traveling' waves). Obviously, the 'monochromatic source' by which the traveling wave is excited according to [17] is, in the one-channel case, the channel wave function ξ_C^E since it causes the alignment of one of the wave functions ϕ_λ in approaching the branch point in the complex energy plane [5]. The traveling waves determine the optical S matrix.

B. Numerical simulation

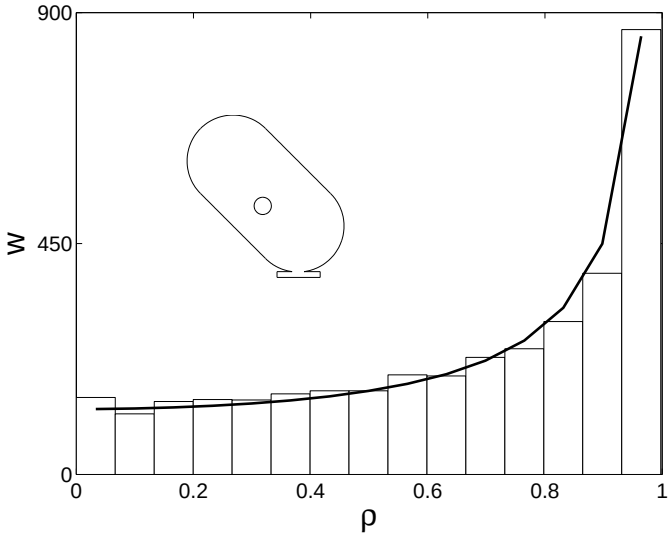

FIG. 4: The ensemble and energy averaged phase rigidity (10) for resonance states of the cavity (c). Energy interval [22, 23]. The full line is calculated from the equation for the phase rigidity distribution in the case of a chaotic cavity with energy averaging and 2 channels [15]. The results for the cavities (a), (b) and (d), see insets in Fig. 2, in the same energy interval [22, 23] as well as those for the cavity (b) in the energy interval [20.5, 21.5] are nearly the same.

The distribution of the phase rigidity is calculated by means of (10). We take the expectation value $\langle\, |\rho|^2 \rangle$ for an ensemble of 200 cavities with different positions of the obstacle in the interior and for 20 different energy values inside the energy interval considered. The results are almost the same in all cases considered, i.e. for the four different open cavities in the energy interval [22, 23] and, in addition, for the cavity (b) in the energy interval [20.5, 21.5]. A typical result is shown in Fig. 4. It agrees well with the theoretical value (full line in Fig. 4) for a chaotic cavity and 2 channels [15]. The phase rigidity is mostly near to its maximum value in the two-channel case. This corresponds to the fact that the transmission is caused by either standing waves or traveling waves with superposed fluctuations. The transition between the two scenarios takes place in a comparably small region according to the examples studied in [9, 18].

IV. SUMMARY

The spectral properties of an open cavity depend strongly on the manner the leads are attached to it. We studied the eigenvalues and eigenfunctions of the effective Hamiltonian $H_{\rm eff}$ describing a large cavity of Bunimovich type with two leads attached in four different ways and one channel in each lead. The transmission is resonant in all cases in relation to the effective Hamiltonian of the open quantum system. In some cases, the transmission takes place via standing waves in the cavity with an intensity that closely follows the profile of the resonances. In other cases, two different types of resonance states appear which differ by their lifetimes. The short-lived states cause traveling modes while the long-lived states appear as fluctuations of the transmission probability. The short-lived states, including the whispering gallery modes, can *not* be identified in the interior of large cavities where the pathway between input and output leads is large. Therefore their widths are relatively small in this case, and it is impossible to identify them in the 'sea' of long-lived resonance states.

The optical S matrix is related to the short-lived states (traveling waves) as can be seen from the eigenvalues and eigenfunctions of $H_{\rm eff}$. This relation is however not necessarily true also in the opposite direction : the eigenvalues of $H_{\rm eff}$ may show separated time scales while the optical S matrix is, nevertheless, small. In such a case, the short-lived modes exist, according to our numerical results, inside the cavity, and their spectroscopic properties are very sensitive against small parameter changes. In the four cases studied by us, ballistic

modes do not appear in the interior of the large chaotic cavity.

In all considered cases, the phase rigidity fluctuates as a function of energy but is mostly near to its maximum value. The distribution is characteristic of the two-channel case.

Acknowledgments

We are indebted to Victor Gopar and Pier Mello for the many discussions on the different possibilities to attach the leads to the Bunimovich stadium. We thank T. Gorin for a critical reading of the manuscript. E.N.B. is grateful to the MPI-PKS for its hospitality during his stay in Dresden. This work has been supported by RFBR grant 05-02-97713 "Enisey".

---

[1] E. Persson, K. Pichugin, I. Rotter and P. Šeba, Phys. Rev. E **58**, 8001 (1998); P. Šeba, I. Rotter, M. Müller, E. Persson and K. Pichugin, Phys. Rev. **61**, 66 (2000); I. Rotter, E. Persson, K. Pichugin and P. Šeba, Phys. Rev. **62**, 450 (2000).

[2] E. Persson, I. Rotter, H.J. Stöckmann and M. Barth, Phys. Rev. Letters **85**, 2478 (2000); H.J. Stöckmann, E. Persson, Y.H. Kim, M. Barth, U. Kuhl, and I. Rotter, Phys. Rev. E **65**, 066211 (2002).

[3] R.G. Nazmitdinov, K.N. Pichugin, I. Rotter, and P. Šeba, Phys. Rev. E **64**, 056214 (2001); Phys. Rev. B **66**, 085322 (2002).

[4] R.G. Nazmitdinov, H.-S. Sim, H. Schomerus and I. Rotter, Phys. Rev. B **66**, 241302(R) (2002).

[5] J. Okołowicz, M. Płoszajczak, and I. Rotter, Phys. Rep. **374**, 271 (2003).

[6] A.F. Sadreev and I. Rotter, J. Phys. A **36**, 11413 (2003).

[7] P. Kleinwächter and I. Rotter, Phys. Rev. C **32**, 1742 (1985).

[8] V.V. Sokolov and V.G. Zelevinsky, Nucl. Phys. A **504**, 562 (1989); Ann. Phys. (NY) **216**, 323 (1992).

[9] I. Rotter and A.F. Sadreev, Phys. Rev. E **69**, 066201 (2004).

[10] A.F. Sadreev, E.N. Bulgakov and I. Rotter, J. Phys. A **38**, 10647 (2005).

[11] R.J. Riddell,Jr., J. Comput. Phys. **31**, 21 (1979) and **31**, 42 (1979).

[12] S. Datta, *Electronic transport in mesoscopic systems*, Cambridge University Press, 1995.

[13] I. Rotter and A.F. Sadreev, Phys. Rev. E **71**, 036227 (2005).

[14] S.A. van Langen, P.W. Brouwer, and C.W.J. Beenakker, Phys. Rev. E **55**, 1 (1997)

[15] P.W. Brouwer, Phys. Rev. E **68**, 046205 (2003).

[16] I. Rotter, Phys. Rev. E **64**, 036213 (2001).

[17] R. Pnini and B. Shapiro, Phys. Rev. E **54**, R1032 (1996).

[18] C. Jung, M. Müller and I. Rotter, Phys. Rev. E **60**, 114 (1999).